Atmos. Chem. Phys. Discuss., 13, 20503–20530, 2013
www.atmos-chem-phys-discuss.net/13/20503/2013/
doi:10.5194/acpd-13-20503-2013


Atmospheric Chemistry and Physics Discussions



# Analyzing time varying trends in stratospheric ozone time series using state space approach

**M. Laine**[1], **N. Latva-Pukkila**[1,2], **and E. Kyrölä**[1]

[1]Finnish Meteorological Institute, Earth Observation Unit, P.O. Box 503, 00101 Helsinki, Finland
[2]Department of Mathematics and Statistics, P.O. Box (MaD), 40014 University of Jyväskylä, Finland

Received: 11 July 2013 – Accepted: 22 July 2013 – Published: 6 August 2013

Correspondence to: M. Laine (marko.laine@fmi.fi)

Published by Copernicus Publications on behalf of the European Geosciences Union.







## Abstract

We describe a hierarchical statistical state space model for ozone profile time series. The time series are from satellite measurements by the SAGE II and GOMOS instruments spanning years 1984–2011. The original data sets are combined and gridded monthly using 10° latitude bands, and covering 25–55 km with 1 km vertical spacing. In the analysis, mean densities are studied separately for 25–35 km, 35–45 km, and 45–55 km layers, also. Model components include level, trend and seasonal effect with solar activity and Quasi-Biennial Oscillations as proxy variables.

We will show how the chosen statistical model is well suited for trend analysis of atmospheric time series that are not stationary but can exhibit both slowly varying and abrupt changes in the distributional properties. The dynamic linear model state space approach provides well defined statistical model for assessing the long term background changes in the ozone time series. The modelling assumptions can be evaluated and the method provides realistic uncertainty estimates for the model based statements on the quantities of interest. We discuss the methodological challenges and practical implementation. The modelling result agree with the hypothesized trend change point for stratospheric ozone at around the year 1997 for mid latitude regions. This is a companion article to Kyrölä et al. (2013).

## 1 Introduction

Time series constructed from satellite remote sensing observations provide important information about variability and trends in the atmospheric chemical compositions. Many satellite time series provide global coverage of the measurement and some of the series are available since the 1980's. The analysis of trends, both natural and human caused, is complicated by natural variability and external forcing affecting stratospheric chemical compositions. In this study, the recovery of stratospheric ozone from the depletion caused by CFC compounds is studied using a statistical time series model.





ACPD
13, 20503–20530, 2013



Slow background changes in stratospheric ozone are easily masked by both seasonal and irregular natural variabilities. This makes stringent requirements for the stability of ozone observations. Self calibrating occultation instruments are good candidates for such a task. The observations analysed in this work consists of satellite measurements by the SAGE II and GOMOS instruments spanning years 1984–2011. The original data sets are combined and gridded monthly using 10° zonal bands, and covering 25–55 km with 1 km vertical spacing. Combining the observations from different instrument having different measurement principles is a challenge. Kyrölä et al. (2013) explains the data set and its construction in more detail. Here the analysis is done both on the 1 km vertical spacing and on 10 km tall mean densities.

There is wealth of literature concerning analysis of atmospheric time series. Standard reference to stratospheric ozone time series regression analysis is SPARC (1998). A recent study that reviews the challenges and problems in trend analysis of climatic time series is by Bates et al. (2012) and general trend analysis reference by Chandler and Scott (2011). For similar type of state space and functional analysis of atmospheric time series that is performed here, see Lee and Berger (2003) and Meiring (2007).

This article studies the feasibility and practical implementation of state space approach for atmospheric time series analysis by describing a dynamic linear model (DLM) for stratospheric ozone time series. Dynamic means here that the regression coefficients can evolve in time. This makes it possible to describe and analyse smooth changes in the average background behaviour of ozone. The model components include level, trend and seasonal effect together with solar activity, and Quasi-Biennial Oscillations (QBO) as proxy variables. We do not claim novelty in the presented methods themselves, but argue that they should be more extensively applied in studying climatic time series and provide a simple framework for time series analyses that can be generalized to more comprehensive studies.In this article, we provide the necessary steps and a computer code for applying the methods.

A typical feature in atmospheric time series is that they are not stationary but exhibit both slowly varying and abrupt changes in the distributional properties. These are





ACPD
13, 20503–20530, 2013



caused by external forcing such as changes in the solar activity or volcanic eruptions. Further, the data sampling is often non uniform, there are data gaps, and the uncertainty of the observations can vary. When observations are combined from various sources there will be instrument and retrieval method related biases. The differences in sampling lead to uncertainties, too. Straightforward linear regression analysis leaves the model residuals correlated as not all variability can be explained by a static linear structure. Usually this is compensated by allowing some correlation structure to the model observation error by using, e.g., autoregressive model. If the residual correlation is not accounted, the model uncertainty analyses are misleading. A simple autoregressive process can explain some of the unmodelled systematic variations by correlated noise, again confusing the analyses. In conclusion, much care in interpretation is needed in order for the standard classical ARIMA type of statistical time series methods to be useful for atmospheric data. A more general approach makes use of dynamic linear models and Kalman filter type of sequential estimation algorithms.

State space models, sometimes called hidden Markov models or structured time series models, are well known and documented in time series literature (Chatfield, 1989; Harvey, 1991; Hamilton, 1994; Migon et al., 2005), modern computationally oriented references are (Durbin and Koopman, 2012) and (Petris et al., 2009). Here, we review the basic properties relevant to the analysis of atmospheric ozone time series data and explain the step necessary to fit the model to seasonal time series and how to assess the uncertainties in the trend estimation.

The structure of this arcticle is the following. The data sets and the statistical model are described in Sect. 2. Results of the statistical time series analyses are given in Sect. 3 and the article ends with discussion and conclusions in Sect. 4.





ACPD
13, 20503–20530, 2013



## 2 Materials and methods

### 2.1 Ozone time series from satellite observations

We use combination of two ozone data sets. The first consists solar occultation measurements of ozone in the stratosphere and lower mesosphere from the SAGE II instrument (Chu et al., 1989) operational during 1984–2005. The second is the GOMOS instrument (Bertaux et al., 2010) that measured ozone in the stratosphere, mesosphere and lower thermosphere in 2002–2012 using stellar occultations. The individual data sets have been combined and homogenized to form a combined time series from 1984 to 2011. The stability of the SAGE II and GOMOS instruments, the construction of the combined time series, data screening, bias correction, and other issues are discussed in more detail by Kyrölä et al. (2013).

### 2.2 Statistical time series model

A general linear state space model with Gaussian errors can be written with observation equation and state evolution equation as

$$\boldsymbol{y}_t = \mathbf{F}_t \boldsymbol{\theta}_t + \boldsymbol{v}_t, \qquad \boldsymbol{v}_t \sim N_p(\mathbf{0}, \mathbf{V}_t), \tag{1}$$

$$\boldsymbol{\theta}_t = \mathbf{G}_t \boldsymbol{\theta}_{t-1} + \boldsymbol{w}_t, \qquad \boldsymbol{w}_t \sim N_q(\mathbf{0}, \mathbf{W}_t), \tag{2}$$

where $\boldsymbol{y}_t$ are the observations and $\boldsymbol{\theta}_t$ is the vector of unobserved states of the system at time $t$. Matrices $\mathbf{F}_t$ and $\mathbf{G}_t$ are the observation operator, that maps the hidden states to the observations and the model evolution operator, giving the dynamics of the states. In this basic formulation the uncertainties are assumed Gaussian, with observation uncertainty covariance $\mathbf{V}_t$ and model error covariance $\mathbf{W}_t$. Above $N_p(\mathbf{0}, \mathbf{V}_t)$ stands for $p$ dimensional Gaussian distributions, with vector of zeros as mean and $\mathbf{V}_t$ as the $p \times p$ covariance matrix. The time index $t$ will go from 1 to $n$, the length of the time series to be analysed. We use notation common to many time series textbooks, e.g. Petris et al. (2009). In the following, the matrices defining the model will mostly be time invariant,





ACPD
13, 20503–20530, 2013



i.e. $\mathbf{G}_t = \mathbf{G}$, etc., and we will usually drop the time subscript, still retaining it in general formulas that are not specific to this particular time series application.

In this work, we use a DLM model to explain variability in the ozone time series with four components: smooth locally linear trend, seasonal effect, effect of external forcing thru proxy variables, and uncorrelated noise. All components are build using the state space approach.

To describe the trend we start with a simple local level and trend model that has two hidden states $\boldsymbol{\theta}_t = [\mu_t, a_t]^T$, where $\mu_t$ is the mean level and $a_t$ is the expected change in the level at time $t$. In addition we need stochastic terms for observational error and for random dynamics of trend and level. These are defined by Gaussian "$\epsilon$" terms below. The system can be written by equations

$$
\begin{aligned}
y_t &= \mu_t + \epsilon_{\text{obs}}, & \epsilon_{\text{obs}} &\sim N\left(0, \sigma^2_{\text{obs}(t)}\right), \quad \text{observations,} \\
\mu_t &= \mu_{t-1} + a_{t-1} + \epsilon_{\text{level}}, & \epsilon_{\text{level}} &\sim N\left(0, \sigma^2_{\text{level}}\right), \quad \text{local level,} \\
a_t &= a_{t-1} + \epsilon_{\text{trend}}, & \epsilon_{\text{trend}} &\sim N\left(0, \sigma^2_{\text{trend}}\right), \quad \text{local trend.}
\end{aligned}
$$

In terms of the state space Eqs. (1) and (2) this is written as

$$
\mathbf{G}_{\text{trend}} = \begin{bmatrix} 1 & 1 \\ 0 & 1 \end{bmatrix}, \quad \mathbf{F}_{\text{trend}} = [10], \quad \mathbf{W}_{\text{trend}} = \begin{bmatrix} \sigma^2_{\text{level}} & 0 \\ 0 & \sigma^2_{\text{trend}} \end{bmatrix}, \quad \mathbf{V}_t = \left[\sigma^2_{\text{obs}(t)}\right]. \tag{3}
$$

As we shall see, depending on the choice of variances $\sigma^2_{\text{level}}$ and $\sigma^2_{\text{trend}}$ this will define a smoothly varying background level of the time series that is used to infer about the changes in atmospheric ozone.

Most atmospheric series exhibit seasonal variability. The seasonality can be modelled using harmonic functions. If the number of seasons is $s$, the full seasonal model has $s/2$ harmonics. For the $k$th harmony, with $k = 1, \ldots s/2$, we need to add two state variables. With monthly data, i.e. $s = 12$, the corresponding blocks of the model and





ACPD
13, 20503–20530, 2013



observation matrices are

$$\mathbf{G}_{\mathrm{seas}(k)} = \begin{bmatrix} \cos(k2\pi/12) & \sin(k2\pi/12) \\ -\sin(k2\pi/12) & \cos(k2\pi/12) \end{bmatrix} \text{ and } \mathbf{F}_{\mathrm{seas}(k)} = [10]. \quad (4)$$

Here the state equation matrices are independent of time index $t$ and we have used subscript $k$ to stand for the harmonic component. We see that $\mathbf{G}_{\mathrm{seas}(k)}$ will rotate a point $[\theta^1, \theta^2]^T$ along a circle using $12/k$ time steps, while the first element, picked by $\mathbf{F}_{\mathrm{seas}(k)}$, varies between two extremes with the season. In our case the seasonality can be adequately explained by two harmonics, e.g. by yearly and half-a-year variation, which will add the number of hidden states to be estimated by four. In addition we need to define the error covariance matrix $\mathbf{W}$ which gives the allowed time-wise variability in the seasonal components.

So far, the state operator $\mathbf{G}$, the observation operator $\mathbf{F}$ and the model error covariance $\mathbf{W}$ have been time invariant. The observation uncertainty covariance $\mathbf{V}_t$ is, in our case, time dependent and it will contain the known observation uncertainties. The inclusion of auxiliary control variables is done by augmenting the observation matrix $\mathbf{F}_t$, making it time dependent. In the following, the stratospheric ozone analysis will utilize three proxy time series explaining parts of the natural variability, one for the solar flux and two proxy variables for Quasi-Biennial Oscillations. This is achieved by adding the following components into the system matrices

$$\mathbf{G}_{\mathrm{proxy}} = \begin{bmatrix} 1\,0\,0 \\ 0\,1\,0 \\ 0\,0\,1 \end{bmatrix} \text{ and } \mathbf{F}_{\mathrm{proxy}(t)} = \begin{bmatrix} x_{1,t} x_{2,t} x_{3,t} \end{bmatrix},$$

where $x_{1,t}$, $x_{2,t}$ and $x_{3,t}$ contain the values of the three proxy series at time $t$. This can be seen as an extension of linear regression analysis into one with time varying parameters. In fact, we could set the corresponding elements of model error covariance matrix $\mathbf{W}$ to zero to obtain time invariant regression coefficients for the proxy variables.





ACPD
13, 20503–20530, 2013



The next step in DLM model construction is the combination of the selected individual model components into larger model evolution and observation equations by

$$\mathbf{G} = \begin{bmatrix} \mathbf{G}_{\text{trend}} & 0 & 0 & 0 \\ 0 & \mathbf{G}_{\text{seas}(1)} & 0 & 0 \\ 0 & 0 & \mathbf{G}_{\text{seas}(2)} & 0 \\ 0 & 0 & 0 & \mathbf{G}_{\text{proxy}} \end{bmatrix}, \quad \mathbf{F} = \left[\mathbf{F}_{\text{trend}} \mathbf{F}_{\text{seas}(1)} \mathbf{F}_{\text{seas}(2)} \mathbf{F}_{\text{proxy}(t)}\right], \tag{5}$$

and the analysis will then proceed to the specification of the variance parameters and to the estimation the model states by state space methods.

## 2.3 Model parameter estimation

After we have defined the model, the next task is the estimation of model parameters given the time series of ozone observations. We have two kinds of unknowns, the model state variables $\boldsymbol{\theta}_t$, one vector for each time $t$, and the parameters that define the model error covariance matrix $\mathbf{W}$, here assumed time independent. At first sight this might seem to be a vastly under determined system, as we have several model parameters for each single observation. However, by the sequential nature of the equations, we can estimate the states by standard recursive Kalman filter formulas.

Implicitly assumed in the state space Eqs. (1) and (2) is that the state at time $t$ in conditionally independent of the history given the previous state at time $t-1$. When the model equation matrices are known, this Markov property allows sequential estimation of the states given the observations by famous Kalman formulas (see e.g. Rodgers, 2000). We can use Kalman filter for one step ahead prediction of the state $p(\boldsymbol{\theta}_{t+1}|\boldsymbol{\theta}_t, \mathbf{y}_{1:t})$ and Kalman smoother for the marginal distribution of the state at time $t$ given the whole time series of observations $p(\boldsymbol{\theta}_t|\mathbf{y}_{1:n})$, for all $t = 1, \ldots, n$. Here marginal means that the uncertainty of the states at all other times that $t$ has been integrated out. These both are needed in time series applications, the filter output can be used to calculate the model likelihood function needed in the statistical analysis, and the Kalman smoother provides an efficient algorithm to estimate and decompose a time





ACPD
13, 20503–20530, 2013



series to parts given in the model formulation. Thus, this large dimensional problem is computationally not much harder than a classical static multiple linear regression analysis. Furthermore, in the linear Gaussian case, the results provided by the Kalman formulas are exact. Non-linear models can be approached by linearization of the state equations, and non-Gaussian error models by, e.g., particle filter algorithms (Doucet et al., 2001).

We describe the Kalman filter step as it is used to calculate model likelihood needed in variance parameter estimation. The Kalman smoother needed for the marginal densities $p(\boldsymbol{\theta}_{1:n}|\boldsymbol{y}_{1:n})$ and the simulation smoother algorithm for sampling from the posterior state both use similar recursive algorithms, whose details can be found in the references (Petris et al., 2009). By the assumed Markov property, the likelihood, i.e. the statistical distribution of the observations given the model states and variance parameters, $p(\boldsymbol{y}_{1:n}|\boldsymbol{\theta}_{1:n})$, can be evaluated sequentially as a product of the individual time wise marginal likelihoods as

$$p(\boldsymbol{y}_{1:n}|\boldsymbol{\theta}_{1:n}) = p(\boldsymbol{y}_1|\boldsymbol{\theta}_1)\prod_{t=2}^{n} p(\boldsymbol{y}_t|\boldsymbol{y}_{1:t-1}, \boldsymbol{\theta}_{1:t}) = \prod_{t=1}^{n} p(\boldsymbol{y}_t|\boldsymbol{\theta}_t). \quad (6)$$

In the case of linear Gaussian model the likelihood becomes proportional to (ignoring a constant that does not depend on the model parameters)

$$p(\boldsymbol{y}_{1:n}|\boldsymbol{\theta}_{1:n}) \propto \exp\left\{-\frac{1}{2}\sum_{t=1}^{n}\left[\left(\boldsymbol{y}_t - \mathbf{F}_t\boldsymbol{\theta}_{\mathrm{p},t}\right)^T \mathbf{C}_{y,t}^{-1}\left(\boldsymbol{y}_t - \mathbf{F}_t\boldsymbol{\theta}_{\mathrm{p},t}\right) + \log\left(|\mathbf{C}_{y,t}|\right)\right]\right\}, \quad (7)$$

where $\boldsymbol{\theta}_{\mathrm{p},t}$ is the one step ahead mean prediction of the state and $\mathbf{C}_{y,t}$ is the covariance matrix of predicted observation, both obtained by the Kalman filter formulas, given below. If we assume that the uncertainty of the state at time $t-1$ is $p(\boldsymbol{\theta}_{t-1}|\boldsymbol{y}_{1:t-1}) = N(\boldsymbol{\theta}_{t-1}, \mathbf{C}_{t-1})$, then the predictive distribution of both parameters and observations and the posterior uncertainty for the state $\boldsymbol{\theta}_t$ at time $t$ after observing $\boldsymbol{y}_t$, i.e. $p(\boldsymbol{\theta}_t|\boldsymbol{y}_{1:t}) = N(\boldsymbol{\theta}_t, \mathbf{C}_t)$, can be calculated with the following formulas (Rodgers,





ACPD
13, 20503–20530, 2013



2000), which consists of first calculating the prior predicted state, its covariance, and the predicted observation covariance as

$$\boldsymbol{\theta}_{\mathrm{p},t} = \mathbf{G}_t \boldsymbol{\theta}_{t-1} \tag{8}$$

$$\mathbf{C}_{p,t} = \mathbf{G}_t \mathbf{C}_{t-1} \mathbf{G}_t^T + \mathbf{W}_t \tag{9}$$

$$\mathbf{C}_{y,t} = \mathbf{F}_t \mathbf{C}_{t-1} \mathbf{F}_t^T + \mathbf{V}_t \tag{10}$$

and then the posterior state and its covariance using the Kalman gain matrix $\mathbf{K}_t$ as

$$\mathbf{K}_t = \mathbf{C}_{p,t} \mathbf{F}_t^T \mathbf{C}_{y,t}^{-1} \tag{11}$$

$$\boldsymbol{\theta}_t = \boldsymbol{\theta}_{\mathrm{p},t} + \mathbf{K}_t (\boldsymbol{y}_t - \mathbf{F}_t \boldsymbol{\theta}_{\mathrm{p},t}) \tag{12}$$

$$\mathbf{C}_t = \mathbf{C}_{p,t} - \mathbf{K}_t \mathbf{F}_t \mathbf{C}_{p,t}. \tag{13}$$

Note that the only matrix inversion required in these formulas is the one related to observation prediction covariance matrix $\mathbf{C}_{y,t}$, which is of size $1 \times 1$ when we analyse univariate time series.

Next, we consider the model error covariance matrix $\mathbf{W}$. If we set all model error variances to zero it will change the DLM model into ordinary, non-dynamic, multiple linear regression model. By using non-zero variances we can fit a smoothly varying mean level, and the smoothness can be controlled by the size of the variances. A typical simplification done here is that we only consider the diagonal elements of $\mathbf{W}$, and even some of these are set to zero. In our case non-zero elements are the second diagonal element for variability in the trend and the variances for seasonal variation, i.e. we will set the level and the three proxy variable variances to zero. The interpretation for the terms as the size of the variability in the change of the states between two time points provides a way to set prior constraints for these value.

A common procedure to estimate the elements of the model error matrix $\mathbf{W}$ is by maximum likelihood method using the likelihood function provided by Eq. (7). After the estimation, the obtained values could be plugged into the system equations as known





ACPD
13, 20503–20530, 2013



constants. The literature on variance parameter estimation is a little vague, as even if the maximum likelihood estimation procedures converges to some value, these parameter do not necessarily identify well and require good subject level knowledge for sensible initial values for the estimation. This plug-in method also neglects the uncertainty in the estimates. Instead of the maximum likelihood, we will use an alternative method based on Bayesian analysis (Gamerman, 2006; Petris et al., 2009) and outline it shortly below.

### 2.4 Markov chain Monte Carlo analysis for variance parameters

The variances in matrix **W** must reflect our prior knowledge on the assumed variability in the process generating the observations. As noted by Gamerman (2006), dynamic linear models offer intuitive means of providing qualitative prior information in the form of the model equations and quantitative information by prior distributions on variance parameters. By using Kalman smoother formulas it is possible to draw samples from the posterior distribution of the states, $p(\boldsymbol{\theta}_{1:n}|\boldsymbol{y}_{1:n})$, given the variance parameter, details e.g. in (Petris et al., 2009). By using so called conjugate priors for the variance parameters, a relatively simple Markov chain Monte Carlo (MCMC) simulation analysis based on Gibbs sampling approach can be set up to draw samples from the joint posterior distribution of the states and the variance parameters (Gamerman, 2006). This can be used to estimate the uncertainty in the variance parameters and also effectively integrate out their uncertainty in the predictive uncertainty analysis of trends. Instead of the Gibbs sampling approach, where one alternates sampling from the state and the model variance parameters, the likelihood of Eq. (7) can be used directly with MCMC to sample from the marginal posterior of **W** according to a Metropolis–Hastings schema, (see e.g. Haario et al., 2006). After obtaining this sample we can, vice versa, sample from the marginal distribution of the state using the simulation smoother, i.e. from the distribution of the states marginalising over the variance parameters. The latter approach requires less samples and provides greater flexibility with respect to the choice of the prior distributions. This approach is used here.





ACPD
13, 20503–20530, 2013



In any case, the estimation procedure tries to find variance parameters that are consistent with the given observation uncertainty, i.e. the model can predict the observations within their accuracy. This means that the scaled prediction residuals that appear in the likelihood formula (Eq. 7) should behave like independent Gaussian variables. We can assess these assumptions by different residual analysis diagnostics.

As we are effectively looking for slowly varying trends in the data, we will set prior constraints to variance parameters to reflect this. For example, we might assume that the change within a month in the background level is on the average some percentage of the overall time series mean. The estimation procedure will then divide the observed variability into model components (level, trend, seasonality) in proportions that reflect the prior choices. The standard model diagnostic tools, such as autocorrelation analysis and normal probability plots reveal possible discrepancies in the model assumptions that have to be considered. As the model residuals are calculated from one step predictions, the diagnostics will reveal both over-fit and a lack-of-fit.

## 2.5 Estimating trends

Trend is a change in the statistical properties of background state of the system (Chandler and Scott, 2011). The simplest case being linear trend, where, when applicable, we only need to specify the trend coefficient and its uncertainty. In the companion article (Kyrölä et al., 2013) the trend and a change in the trend is studies by using a "V" shaped piecewise linear model with predefined change point in time. Natural systems evolve continuously in time and it is not always appropriate to approximate the background evolution with a constant, or piecewise linear, trend. Within the state space dynamic linear model framework, the trend can be defined as the change in the estimated background level. However, the trend component $a_t$ in our DLM formulation, describes local change in the level, and might not directly be "the trend" we are looking for. Posterior sampling from the background level provides efficient method for studying uncertainties in different trend estimates.





ACPD
13, 20503–20530, 2013



Trend analysis can be a delicate matter and it is always challenging to give causal explanations. With a properly set up and estimated DLM model we can detect smooth changes in the background state. By using proxy variables we can filter out the effect of known external forcing, such as the solar effect. The DLM analysis provides a method to detect and quantify trends, but the statistical model itself does not provide explanations. It can say that the observations are consistent with selected model. Model diagnostics will eventually falsify wrong models and other badly selected prior specifications.

Temporal changes in the system can be studied by visually inspecting the background level and its estimated uncertainty. We can draw samples from the posterior distribution of the level to asses hypotheses about the evolution of the process. For example, study the average change in the mean in 10 yr periods, as done in Sect. 3. We take into account the uncertainty in model prediction and in the estimated variance parameters by sampling possible background levels from the posterior uncertainty distribution. We will do this consecutively, and for each sample calculate the ten year change in the mean.

In our analyses, MCMC is used to sample from both state space and model parameter uncertainty distribution. This provides a simple way of accounting for both state space and variance parameter uncertainty in the analyses of trends. The procedure is the following:

1. Produce a sample of the variance parameters defining the error covariance matrix **W** using Metropolis–Hastings MCMC with Kalman filter likelihood defined in Eq. (7).

2. Draw one realization of matrix **W** from its posterior distribution provided by MCMC in the previous step.

3. Draw one realization of model state $\boldsymbol{\theta}_{1:n}$ using the Kalman simulation smoother assuming fixed **W** from the previous step and calculate trend related statistic of interest from this realization.





ACPD
13, 20503–20530, 2013



4. Repeat from step 2. to calculate summaries from the posterior distribution of the quantity of interest.

In Sect. 3 this method is used to calculate 10 yr trend and trends before and after the year 1997 with uncertainty estimates.

### 2.6 Some technical notes

The recursive Kalman formulas depend on known distribution for the initial time uncertainty at $t = 1$, $p(\boldsymbol{\theta}_1)$. It is possible to derive exact formulas for estimating this distribution when the prior information is diffuse, i.e. the prior uncertainty grows without a limit. Alternatively, an accurate approximation is achieved by using two pass algorithm, where a large uncertainty at $t = 1$ in the first pass is replaced by the Kalman smoother provided uncertainty in the second pass.

In this study, we will assume that the model error $\mathbf{W}_t = \mathbf{W}$ is time invariant. If we think that this assumption is not be feasible, we could set up an additional DLM hierarchy of parameters that define the evolution of $\mathbf{W}_t$ and still stay in the DLM framework.

The DLM model analysis is based on standard Kalman filter algorithms and as such can be programmed by most numerical analysis software such as Matlab or by using the statistical language R. Some additional effort is needed for the parameter estimation by MCMC. Here we have used Matlab and checked the results with the R package DLM (Petris et al., 2009). The Matlab code we used for the DLM analyses including the MCMC part is available from http://helios.fmi.fi/~lainema/dlm/.

## 3 Results and discussion

In this section we apply the state space DLM approach for modelling trends in satellite observations of stratospheric ozone. The model is similar to more classical linear regression models used for ozone time series by Kyrölä et al. (2013) and previously, e.g., by SPARC (1998). Our analysis is an extension to those regression models, as





ACPD
13, 20503–20530, 2013



the DLM model allows time variation in the regression coefficients. The amount of this time variation is defined by the variance parameters which are estimated from the data.

We use locally linear trend model with 2 harmonic functions for the seasonal effect and three proxy time series for the solar flux and Quasi-Biennial Oscillations. These proxies are the same as in Kyrölä et al. (2013). The model error covariance **W** is time invariant, with nonzero diagonal terms for the trend parameter and a common value for the four parameters defining the variability in the seasonal components. Prior distribution for standard deviation of yearly level change was set as log-normal with mean equal to 0.06 % of the mean level of the observations and having 80 % standard deviation. For seasonal standard deviation the numbers were 10 % and 50 %. By this setup, most of the modelled variations are attributed to the seasonal effect.

The simple parameterization of the model error term with only two unknown parameters was selected by performing initial fits with different parameterizations, using sensible initial values refined by a maximum likelihood optimization. The models were then diagnosed by studying the residuals by normal probability plots and autocorrelation function estimates. When a good candidate model was found, a Markov chain Monte Carlo (MCMC) analysis was used to study the uncertainty and identifiability of the variance parameters. Lastly, the interesting trend features of the time series were studied by plotting the estimated background level with uncertainty confidence bounds, and drawing simulations from the posterior distribution of the level term and checking the statistical significance of hypothesized features. Here statistical significance means the relative width of predictive posterior probability distribution of the quantity of interest.

The model parameters have been fitted separately to each data set, i.e. to each height interval and zonal band. We performed the analyses using vertical average profile data with both 1 km altitude grid and by summing them to obtain averaged densities for three altitude regions: 25–35 km, 35–45 km, and 45–55 km. The zonal bands start from 60° S and go to 60° N at 10° spacing. The denser altitude grid was used to provide





ACPD
13, 20503–20530, 2013



trend maps comparable to those by Kyrölä et al. (2013) and the combined altitudes were used to make more global trend analysis.

Initially, a multivariate estimation was considered, also, where several altitudes and zonal bands are fitted together, but we did not gain additional insight into the data. By considering each zonal band independently and summing several altitudes, we have tried to reduce the model to a minimum one that still shows interesting long term distributional changes and is consistent with the modelling assumptions. The opposite methodological direction would be to use the observations in more refined resolution and model several time series in one estimation step, using individual satellite retrievals instead of spatial-temporal averages. This could benefit the understanding of the spatial and temporal dependence of the changes. The ultimate step would be the assimilation of the satellite observations to an atmospheric model.

Figure 1 shows modelling results in one altitude-latitude region, 40° N–50° N, 35–45 km. The original data is displayed together with the Kalman smoother based estimate and with the model level component that is used to infer about the trend. Separate panel on lower left displays the 10 yr trend obtained from the level component using MCMC analysis to account for the uncertainty in the variance parameters. After the DLM decomposition the model residual term is assumed to be uncorrelated Gaussian noise. The two lower right panels in Fig. 1 show residual diagnostics. These are used to to look for deviations from the modelling assumptions. If the scaled residuals pass the check of being independent and Gaussian with unit variance, then the fit agrees with our assumptions and modelling results are consistent with the data.

Figure 2 shows the fitted model components for 40° N–50° N, 35–45 km. Each model component is shown with a 95 % uncertainty enveloped. In the second up-most panel solid back lines are samples from possible realization of the model's level component, obtained by MCMC, that is used to infer about the trend. Also, as a result from MCMC analysis, Fig. 3 shows the prior standard deviation together with estimated marginal posterior distributions for the two variance parameters for the same data set. The local change in the level is more constrained by the chosen prior compared to seasonal





ACPD
13, 20503–20530, 2013



effect, which was deliberately done to support the search for smooth background variability.

In Fig. 4 the results of ten year trend analyses are collected and plotted separately for the three altitude ranges. The colouring shows the trend, i.e. the average change in ±5 yr around the time axis point. Blue colour means negative and red positive trend. The change is most visible in upper altitudes 45–55 km and 35–45 km. In the lower altitudes, 25–35 km there are some visible changes, but it is mostly masked by larger variability and noise due to the lesser quality of satellite observations at these altitudes.

Kyrölä et al. (2013) analysed the trend change point by calculating several fixed piecewise linear regression analyses and choosing the one that provided largest difference between before and after the point change in the linear trend. In the DLM approach the trend can change its value continuously and we can analyse directly where the most likely change points are. One use of a DLM model would be the identification of possible trend change points, and provide hypotheses on which a traditional static regression analysis would be performed. The results of linear "V" shape trend analysis in Kyrölä et al. (2013) are mostly in agreement with the results here. We performed same trend analysis using the DLM approach, i.e. studied the difference in trend between the years from 1984 to 1997 and from 1997 to 2011. Figure 16 by Kyrölä et al. (2013) corresponds to our Fig. 5. These two figures are very close to each other. This is quite remarkable as the DLM analysis is much more flexible than the hockey stick model used by Kyrölä et al. (2013).

One particular feature of interest in the data is the suggested stratospheric ozone recovery due to prohibition of CFC compounds by the Montreal treaty in 1987. Several studies indicate a possible turning point around year 1997 (Newchurch et al., 2003; Jones et al., 2009; Steinbrecht et al., 2009). According to our analyses, significant changes in the average background level of ozone can be seen at mid-latitudinal regions 40° S–20° S and 20° N–40° N and in the altitude range 35–55 km. At these regions the trend, measured as average change in ten years, has turned from negative to positive before the year 2000. Further, in those geographical regions where the "V" type of





ACPD
13, 20503–20530, 2013



description of the change is appropriate, the turning point is around years 1997–1998. The change points and trend features have slight variations by latitude and altitude. In some regions there are signs of reduction of ozone after the year 2007. Near equator the long time background changes are masked with irregular variations in the ozone concentration.

Finally, all the data sets and the modelled ozone levels for the 12 analysed 10° zonal bands at three 10 km tall altitude layers are collected in Figs. 6 and 7.

## 4 Conclusions

Dynamic linear models (DLM) are well suited for modelling atmospheric time series. In contrast to some classical time series analyses, they do not require stationarity, they allow for missing observations and take into account the uncertainty in the observations. By using Markov chain Monte Carlo (MCMC) simulation analysis, the uncertainty in the structural variance parameters can be accounted in the results. The state space methods directly include a model error term, which makes the analysis more robust to mis-specification of the model. The analysis allows full statistical uncertainty quantification, and it is extendible to more refined analyses, if those seem necessary. Here, a relatively straightforward and conceptually simple analysis reveals interesting features and, also, validates the more ad hoc choices used in piecewise linear global analyses, such as in the companying paper by Kyrölä et al. (2013).

The results show that the combined SAGE II-GOMOS time series comprise statistically significant change point approximately after year 1997 at altitudes 35–55 km and mid latitudes, between 50° S–20° S and 20° N–50° N. This change point location has slight variation by latitude and altitude. This result is in agreement with other studies and signals the recovery of the ozone layer. However, there are locations where the changes are estimated opposite to the expected. The length of the series is still short relative to some cycles of natural variability in the atmospheric processes. The start of





ACPD
13, 20503–20530, 2013



a period for increased solar activity from 2012 will make the observations from next few coming years an important verification for the results.

*Acknowledgements.* This research has been supported by the Academy of Finland MIDAT project and by project number 132808.

## References

Bates, B. C., Chandler, R. E., and Bowman, A. W.: Trend estimation and change point detection in individual climatic series using flexible regression methods, J. Geophys. Res., 117, D16106, doi:10.1029/2011JD017077, 2012. 20505

Bertaux, J. L., Kyrölä, E., Fussen, D., Hauchecorne, A., Dalaudier, F., Sofieva, V., Tamminen, J., Vanhellemont, F., Fanton d'Andon, O., Barrot, G., Mangin, A., Blanot, L., Lebrun, J. C., Pérot, K., Fehr, T., Saavedra, L., Leppelmeier, G. W., and Fraisse, R.: Global ozone monitoring by occultation of stars: an overview of GOMOS measurements on ENVISAT, Atmos. Chem. Phys., 10, 12091–12148, doi:10.5194/acp-10-12091-2010, 2010. 20507

Chandler, R. E. and Scott, E. M.: Statistical Methods for Trend Detection and Analysis in the Environmental Sciences, John Wiley & Sons, 2011. 20505, 20514

Chatfield, C.: The Analysis of Time Series, an Introduction, 4th edn., Chapman & Hall, 1989. 20506

Chu, W. P., McCormick, M. P., Lenoble, J., Brogniez, C., and Pruvost, P.: SAGE II inversion algorithm, J. Geophys. Res., 94, 8339–8351, 1989. 20507

Doucet, A., Freitas, N., and Gordon, N.: Sequential Monte Carlo Methods in Practice, Statistics for Engineering and Information Science, Springer, 2001. 20511

Durbin, T. and Koopman, S.: Time Series Analysis by State Space Methods, Oxford Statistical Science Series, 2nd edn., Oxford University Press, 2012. 20506

Gamerman, D.: Markov Chain Monte Carlo – Stochastic Simulation for Bayesian Inference, 2nd edn., Chapman & Hall, 2006. 20513

Haario, H., Laine, M., Mira, A., and Saksman, E.: DRAM: Efficient adaptive MCMC, Stat. Comput., 16, 339–354, doi:10.1007/s11222-006-9438-0, 2006. 20513

Hamilton, J. D.: Time Series Analysis, Princeton University Press, 1994. 20506

Harvey, A. C.: Forecasting, Structural Time Series Models and the Kalman Filter, Cambridge University Press, 1991. 20506





ACPD

13, 20503–20530, 2013



Jones, A., Urban, J., Murtagh, D. P., Eriksson, P., Brohede, S., Haley, C., Degenstein, D., Bourassa, A., von Savigny, C., Sonkaew, T., Rozanov, A., Bovensmann, H., and Burrows, J.: Evolution of stratospheric ozone and water vapour time series studied with satellite measurements, Atmos. Chem. Phys., 9, 6055–6075, doi:10.5194/acp-9-6055-2009, 2009. 20519

Kyrölä, E., Laine, M., Sofieva, V., Tamminen, J., Päivärinta, S.-M., Tukiainen, S., Zawodny, J., and Thomason, L.: Combined SAGE II-GOMOS ozone profile data set 1984–2011 and trend analysis of the vertical distribution of ozone, Atmos. Chem. Phys. Discuss., 13, 10661–10700, doi:10.5194/acpd-13-10661-2013, 2013. 20504, 20505, 20507, 20514, 20516, 20517, 20518, 20519, 20520, 20528

Lee, J. and Berger, J. O.: Space-time modeling of vertical ozone profiles, Environmetrics, 14, 617–639, doi:10.1002/env.608, 2003. 20505

Meiring, W.: Oscillations and time trends in stratospheric ozone levels: a functional data analysis approach, J. Am. Stat. Assoc., 102, 788–802, doi:10.1198/016214506000000825, 2007. 20505

Migon, H. S., Gamerman, D., Lopes, H. F., and Ferreira, M. A.: Dynamic models, in: Handbook of Statistics, vol. 25, Bayesian Thinking: Modeling and Computation, Elsevier, 553–588, doi:10.1016/S0169-7161(05)25019-8, 2005. 20506

Newchurch, M. J., Yang, E.-S., Cunnold, D. M., Reinsel, G. C., Zawodny, J. M., and Russell, J. M.: Evidence for slowdown in stratospheric ozone loss: First stage of ozone recovery, J. Geophys. Res.-Atmos., 108, 4507, doi:10.1029/2003JD003471, 2003. 20519

Petris, G., Petrone, S., and Campagnoli, P.: Dynamic Linear Models with R, Use R!, Springer, , 2009. 20506, 20507, 20511, 20513, 20516

Rodgers, C. D.: Inverse Methods for Atmospheric Sounding: Theory and Practice, World Scientific, World Scientific Publishing Company is headquartered in Singapore, 2000. 20510, 20511

SPARC: Assessment of Trends in the Vertical Distribution of Ozone, Tech. Rep. 43, World Meteorological Organization Global Ozone Research and Monitoring Project, wCRP-SPARC Report 1, 1998. 20505, 20516

Steinbrecht, W., Claude, H., Schonenborn, F., McDermid, I. S., Leblanc, T., Godin-Beekmann, S., Keckhut, P., Hauchecorne, A., van Gijsel, J. A. E., Swart, D. P. J., Bodeker, G. E., Parrish, A., Boyd, I. S., Kampfer, N., Hocke, K., Stolarski, R. S., Frith, S. M., Thomason, L. W., Remsberg, E. E., von Savigny, C., Rozanov, A., and Burrows, J. P.: Ozone and temperature trends in the upper stratosphere at five stations of the network for





ACPD
13, 20503–20530, 2013



the detection of atmospheric composition change, Int. J. Remote Sens., 30, 3875–3886, doi:10.1080/01431160902821841, 2009. 20519





ACPD
13, 20503–20530, 2013



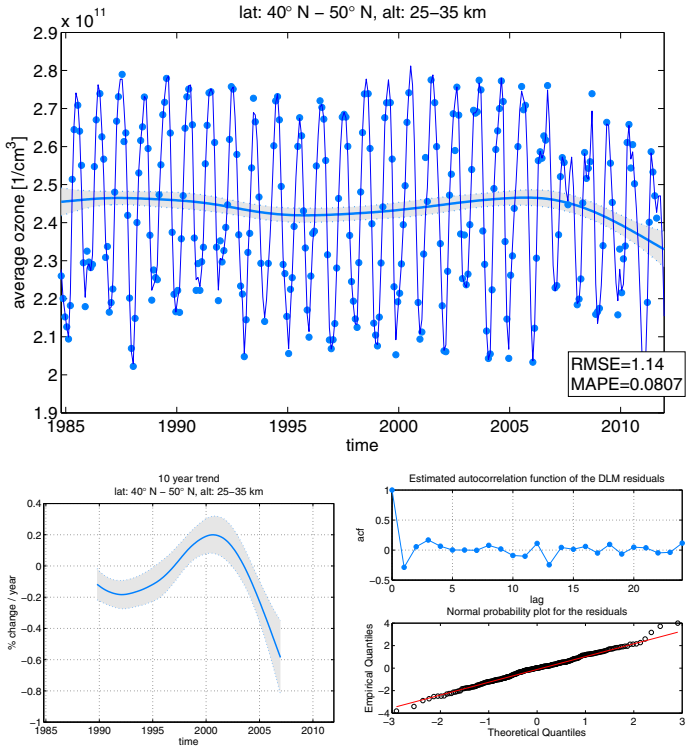


**Fig. 1.** DLM fit for average ozone at 40° N–50° N, 35–45 km. In upper panel the dots are the observations used in the analysis, solid line following the observations is the DLM fit obtained by Kalman smoother. RMSE refers to root mean square error of the scaled residuals, MAPE is mean absolute relative prediction error, i.e. the relative amount of variation in the data not explained by the model. The smooth solid line is the background level component of the model with 95 % probability envelope. In lower left panel analysis of the 10 yr trend is performed. Lower right panel shown model diagnostic analyses on the residuals by estimated autocorrelation function and by normal probability plot.





ACPD
13, 20503–20530, 2013



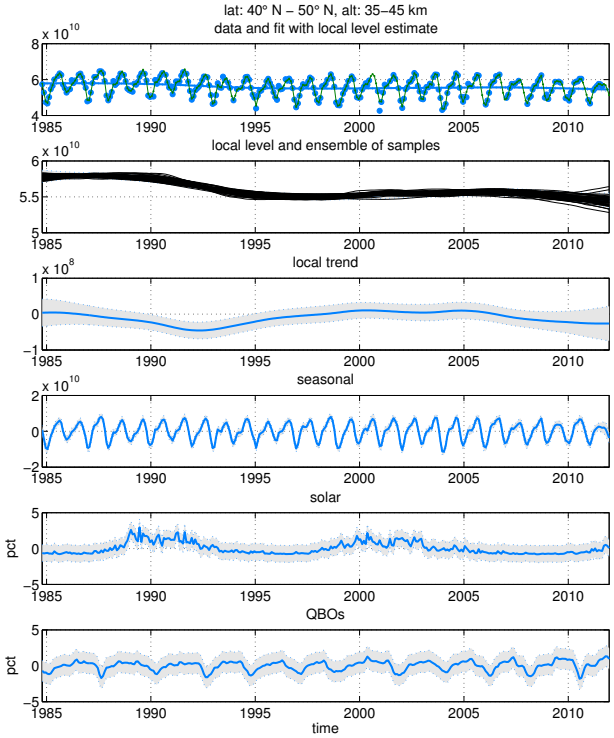


**Fig. 2.** DLM model components for one selected zonal band and altitude region. First panel corresponds to that in Fig. 1, with same latitude and altitude. Second panel shows the level component overlayed with an ensemble of simulations from the combined state end variance parameter posterior. The other panels show means and 95 % probability envelopes of the remaining DLM components, trend, seasonal, solar and Quasi-Biennial Oscillations.





ACPD
13, 20503–20530, 2013



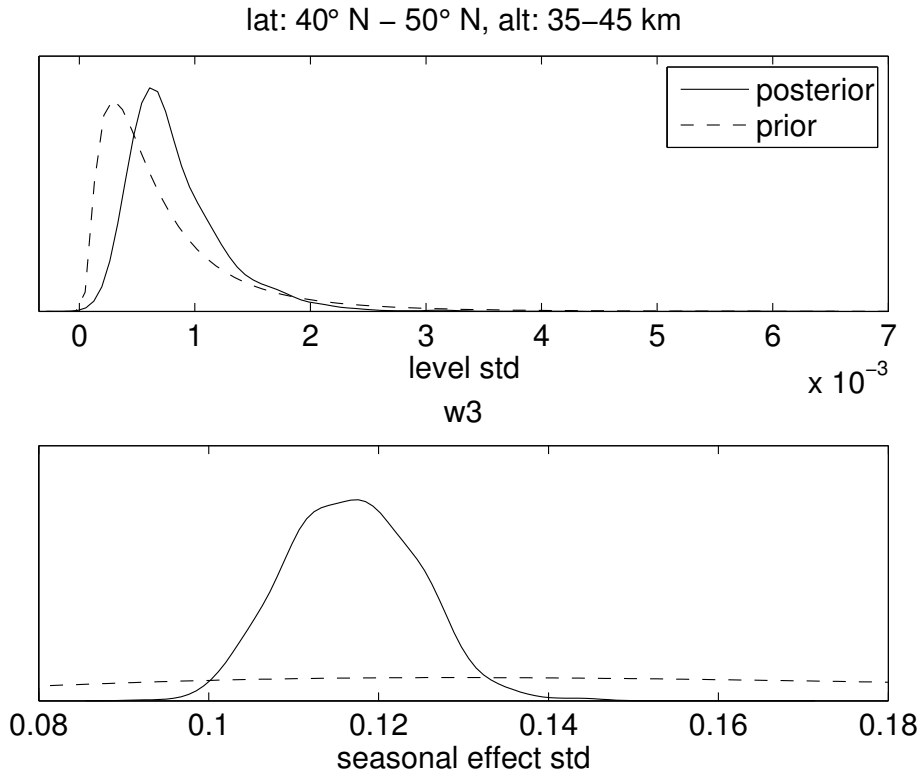


**Fig. 3.** Marginal prior and posterior densities for standard deviation defining the two values in the diagonal of model error matrix **W**. The posterior is obtained by MCMC simulation analysis.





ACPD
13, 20503–20530, 2013



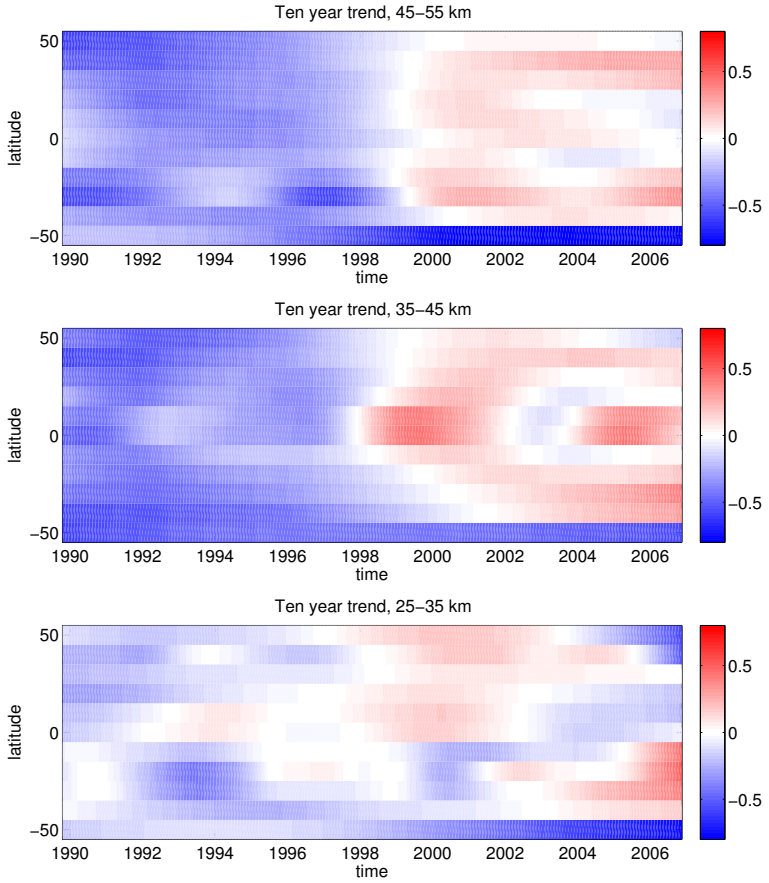


**Fig. 4.** Ten-year trend in percentage change/year from the DLM fits for each altitude region and zonal band. One individual trend analysis is shown in the lower left panel of Fig. 1.





ACPD
13, 20503–20530, 2013



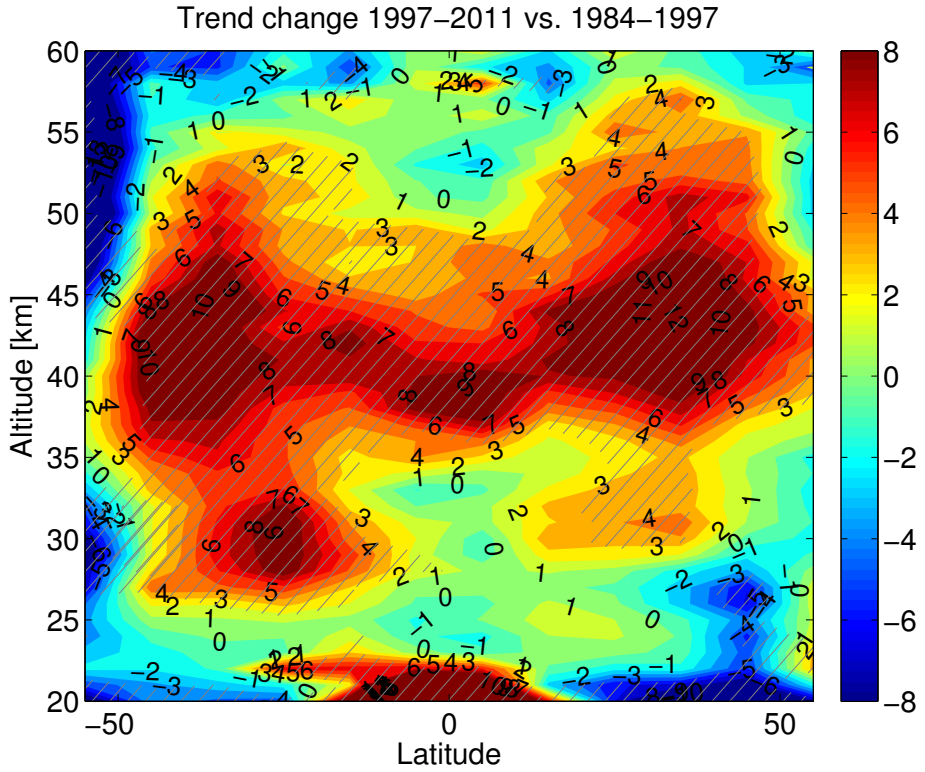


**Fig. 5.** To compare DLM results to linear regression analysis in Kyrölä et al. (2013) we reproduce its Fig. 16. The change in ozone trends in % per decade between the periods 1997–2011 and 1984–1997. Shaded area are approximately those where the trend difference is non zero with over 95 % posterior probability.





ACPD
13, 20503–20530, 2013



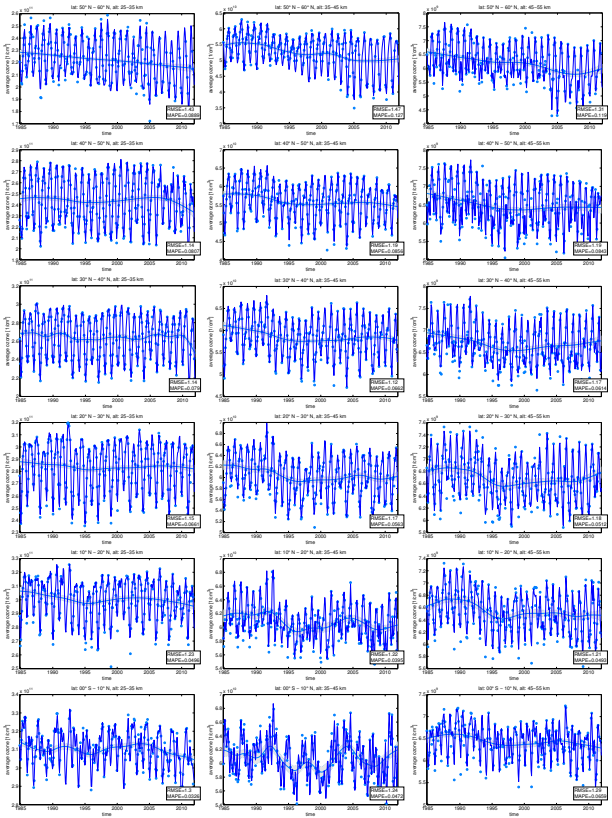

**Fig. 6.** All fits collected, Northern Hemisphere. The three altitude regions as columns, Northern Hemisphere 10° zonal bands as rows starting from the north most zone. Smooth solid curve is the estimated background level with 95 % probability envelope. The dots are observations used in the analysis. The solid line following the observations is the DLM fit obtained by Kalman smoother formulas.





ACPD
13, 20503–20530, 2013



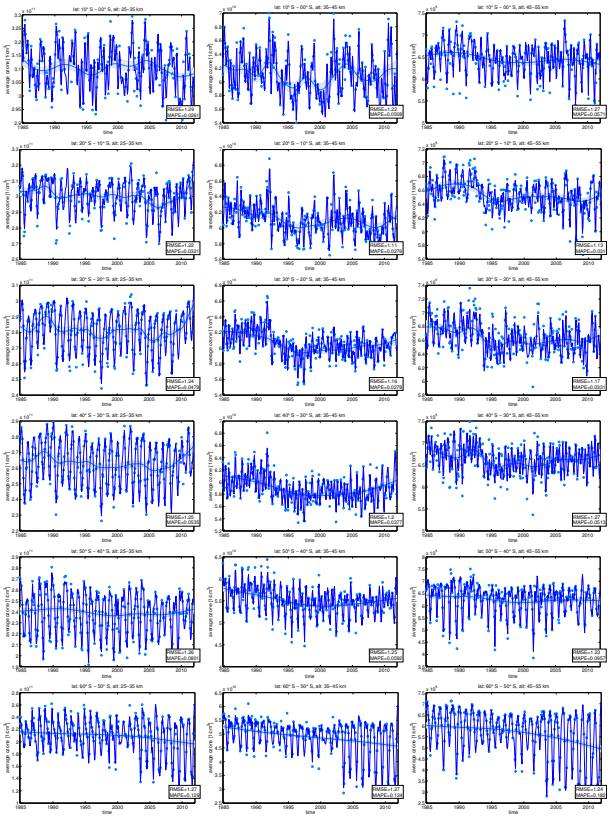

**Fig. 7.** All fits collected, Southern Hemisphere. The three altitude regions as columns, Southern Hemisphere 10° zonal bands as rows starting from the equatorial zone. See Fig. 6 for explanation.





ACPD
13, 20503–20530, 2013